Histol Histopathol (2015) 30: 737-749
DOI: 10.14670/HH-30.737

http://www.hh.um.es

Histology and Histopathology
Cellular and Molecular Biology

Beneficial effects of cannabinoid receptor type 2 (CB2R) in injured skeletal muscle post-contusion

Tianshui Yu[1,2,3], Xu Wang[2,3], Rui Zhao[1], Jilong Zheng[1], Liqiang Li[1], Wenxiang Ma[1], Shutao Zhang[1] and Dawei Guan[1]

[1]Department of Forensic Pathology, China Medical University School of Forensic Medicine, Shenyang, China [2]Collaborative Innovation Center of Judicial Civilization and [3]Key Laboratory of Evidence Science, China University of Political Science and Law, Ministry of Education, Beijing, China

Summary. The aim of the current study was to investigate the effects of cannabinoid receptor type 2 (CB2R) on the repair process of injured skeletal muscle, which could potentially lay solid foundations as a novel target for curing muscular fibrosis in future. A standardized rat model of skeletal muscle contusion was established, where rats were treated with the CB2R agonist JWH-133 or antagonist AM-630. The *in vivo* results revealed that CB2R activation with JWH-133 significantly diminished the fibrotic areas, down-regulated the mRNA levels of collagen type I/III and augmented the number of multinucleated regenerating myofibers in the injured zones. The reasons leading to the aforementioned results were directly attributable to decreased mRNA levels of TGF-β1, FN-EIIIA and α-SMA, reduced accumulation of myofibroblasts, and concomitantly increased mRNA levels of matrix metalloproteinase-1/2. However, we observed contrasting changes in rats treated with the CB2R antagonist AM-630. These results revealed multiple effects of CB2R in systematically inhibiting fibrotic formation and improving muscle regeneration, alongside its potential for clinical application in patients with skeletal muscle injuries and diseases.

Key words: Muscle injury, Fibrosis, Regeneration, Cannabinoid receptor type 2 (CB2R)

Offprint requests to: Dawei Guan, M.D., Ph.D., Department of Forensic Pathology, China Medical University School of Forensic Medicine, No. 77, Puhe Road, Shenbeixin District, Shenyang 110122, Liaoning Province, China. e-mail: dwguan2014@126.com

Introduction

Muscle injury presents challenges in the fields of sports medicine, traumatology and forensic pathology, due to the time-intensive healing of injured muscles and incomplete functional recovery that often occurs, depending on the severity of the initial trauma. Injured skeletal muscle has the profound ability to regenerate through a highly coordinated sequence of events, largely attributed to the activation of the muscle progenitor cells and their fusion into mature multinucleated myofibers. Nevertheless, the gradual development of fibrotic scarring within the injured area hinders muscle regeneration by 1) presenting a mechanical barrier to cell migration and fusion, 2) providing inappropriate signals for cell differentiation, and 3) limiting vascular perfusion of the injured site; this ultimately results in an incomplete functional recovery. The fibrogenic process in fibrotic cascades is characterized by the up-regulation of the fibrogenic cytokine transforming growth factor-β1 (TGF-β1), fibronectin extra domain A (FN-EIIIA) and the intense accumulation of myofibroblasts. Myofibroblasts, as highly synthetic collagen fibers, are characterized by a contractile phenotype and the presence of alpha-smooth muscle actin (α-SMA) stress fibers (Lotersztajn et al., 2005). Besides, matrix metalloproteinase-1/2 (MMP-1/2) are two important enzymes that regulate the synthesis and degradation of the extracellular matrix (ECM) in the remodeling process of fibrotic cascades. However, little research has been conducted on the development of fibrotic cascades in skeletal muscle. Therefore, enhanced understanding of the crucial role of the targets in the pathway of fibrotic

cascades is a prerequisite for the identification of the antifibrotic targets, and the subsequent development of antifibrotic drugs. The long-term goal of our study is to identify antifibrotic targets, and enforce biological interventions to inhibit muscle fibrosis and promote improved muscle regeneration.

A novel endogenous signaling pathway was identified by the discovery of specific membrane receptors of the marijuana component Δ^9-tetrahydrocannabinol (Δ^9-THC) in the early 1990s, now referred to as the endocannabinoid system (Felder et al., 1992). The endogenous cannabinoid system comprises the cannabinoid receptor type 1 and 2 (CB1R and CB2R, respectively), their endogenous ligands (endocannabinoids) and the enzymes that synthesize and degrade endocannabinoids. CB1R and CB2R have been cloned and characterized, respectively (Matsuda et al., 1990; Munro et al., 1993). Belonging to the 'seven transmembrane spanning receptors' family, both cannabinoid receptors are coupled to G proteins (particularly those of the $G_{i/o}$ family), which are activated by cannabinoid Δ^9-tetrahydrocannabinol (Δ^9-THC), as well as by endocannabinoids such as arachidonoylethanolamide (AEA or anandamide) or 2-arachidonoylglycerol (2-AG) (Di Marzo, 1998; Pertwee, 2001; McAllister and Glass, 2002; Bisogno et al., 2005).

As previously reported (Cavuoto et al., 2007), CB2R was expressed in both human and rodent skeletal muscle tissue. Recently, we also found that CB2R was highly induced in the injured skeletal muscle tissue of rats, and in macrophages and spindle-shaped fibroblastic cells at the injured sites (Yu et al., 2010). Nevertheless, its effects on the repair of injured skeletal muscle remain unclear. General consensus holds that CB2R exerts anti-fibrosis effects in diverse organ types. For instance, CB2R activation abrogates the fibrotic process by arresting growth and triggering the apoptosis of myofibroblasts in human cirrhotic liver *in vitro* (Julien et al., 2005). Moreover, the selective CB2R agonist JWH-133 regresses fibrosis in cirrhotic rats with apoptosis of hepatic myofibroblasts (Muñoz-Luque et al., 2008). Consequently, pharmacological intervention of the hepatic endocannabinoid pathway offers potential for the treatment of liver fibrosis. In addition, CB2R activation may protect against post-ischemia/reperfusion heart failure through direct inhibition of cardiac myocyte death and prevention of myofibroblast activation (Defer et al., 2009). Treating mice through JWH-133 also prevents the profibrotic effect of bleomycin in the skin, while inhibition of CB2R signaling augments bleomycin-induced dermal fibrosis (Akhmetshina et al., 2009). Besides, CB2R is also involved in the control of skin and lung fibrosis, and of autoimmunity in a mouse model of systemic sclerosis (SSc) induced by hypochlorite (Servettaz et al., 2010). Therefore, we established an animal model of skeletal muscle contusion to test the hypothesis that CB2R plays a significant role in fibrosis and regeneration during the repair of injured skeletal muscle in rats, which may promote understanding for CB2R as a novel target to resolve skeletal muscle injuries and diseases.

Materials and methods

Animal model of skeletal muscle contusion

All animal protocols conformed to the "Principles of Laboratory Animal Care" (National Institutes of Health, Published No. 85-23, Revised 1985) (with the intention to minimize both the number of animals used, and any suffering they might experience), and were performed according to China Medical University's Guidelines for the Care and Use of Laboratory Animals. As previously described, a reproducible muscle contusion model in rats was used (Yu et al., 2010; Zhang et al., 2013). Briefly, a total of 20 healthy, adult Sprague-Dawley male rats weighing between 230 and 250 g were anesthetized by intraperitoneal injection with 2% sodium pentobarbital (30 mg/kg). The rat's right hindlimb was positioned on a board in a prone position by extending the knee and dorsiflexing the ankle to 90°, before a single impact was delivered to the gastrocnemius and soleus muscles of the right posterior limb. The center of the contusion was marked to help define the injection site. Each rat was individually housed in a cage and fed regular laboratory chow, while water was supplied *ad libitum*. A 12-hour day and night cycle was maintained. In order to remove muscle samples from the wound sites for morphological evaluation, 5 rats were sacrificed by intraperitoneal injection of an overdose of sodium pentobarbital (350 mg/kg) at 14 days post-injury. No bone fractures were detected during dissection. The remaining 15 rats were treated and evaluated as described below.

Treatment with the CB2R agonist or antagonist

Of the 20 rats, 15 were randomly divided into 3 groups (five rats per group) according to different treatments with JWH-133 (Tocris Bioscience, Ellisville, MO, USA), AM-630 (Tocris Bioscience, Ellisville, MO, USA) or Vehicle alone, post-creation of injury. JWH-133 and AM-630 were dissolved in DMSO, aliquoted, and stored as stock solutions at a concentration of 12.5 mg/ml at -20°C. The working solution was freshly prepared prior to injection by diluting the stock solutions in NaCl at the concentration of 5 mg/ml and total volume of 50 μl, and then injected intramuscularly into the injection site of each injured right hindlimb per rat at 0 h, 1 day, 3, 5, 7, 9, 11 and 13 days post-injury, respectively. Those rats injected with equal volumes of Vehicle were used as controls. Fourteen days after injury, all animals were killed by intraperitoneal injection of an overdose of sodium pentobarbital (350 mg/kg). Next, post-treated muscle samples were removed from the wound sites, and fixed in 4% paraformaldehyde in phosphate-buffered saline (pH 7.4) for histopathological and immunohistochemical analysis, or stored at -80°C for determination of mRNA.

Histopathological staining and morphometric analysis

Fixed muscle specimens were embedded in paraffin. A 5-μm-thick tissue section was prepared from the paraffin-embedded tissue and stained with either hematoxylin and eosin (H&E), or with Masson's trichrome staining.

The H&E staining was examined histologically for quantification of regenerating muscle fibers within the injured sites treated with JWH-133, AM-630 or Vehicle, before the results were compared among the different groups. Centronucleated myotubes (the hallmark of skeletal muscle regeneration) were considered to be regenerating myofibers (Goetsch et al., 2003), while nuclei with no discernible surrounding cytoplasm were discarded. Six microscopic fields were randomly selected at 400-fold magnification in each section, with the number of regenerating myofibers within the injured sites counted by bright field microscopy. The average number of regenerating myofibers in the 6 randomly chosen visual fields was calculated as the result of each wound specimen.

Masson's trichrome staining was used for the detection of collagen accumulation at the wound sites, with or without treatment, with the collagen deposition presenting as blue color in the sections. The fibrotic area (expressed as a percentage of the wound area) was assessed by analyzing the 6 fields of Masson's trichrome-stained skeletal muscle sections per animal. Each field was acquired at 400-fold magnification and morphometrical analysis was performed using Image-Pro Plus 6.0 (Media Cybernetics, USA).

Finally, all the measurements and data analyses were performed independently and in a blinded manner by two pathologists.

Immunohistochemical staining and morphometric analysis

Immunostaining was performed using the streptavidin-peroxidase method. Briefly, tissue sections post-treatment were mounted on APES-coated glass slides. The sections were deparaffinized in xylene, rehydrated with a series of graded alcohol, and then heated in 0.01 mol/L sodium citrate buffer (pH 6.0) with a medical microwave oven for antigen retrieval. Subsequently, 3% hydrogen peroxide was applied for quenching endogenous peroxidase activity. The sections were blocked with 10% non-immune goat serum to reduce non-specific binding, before the tissue sections were then incubated with mouse anti-α-SMA monoclonal antibodies (dilution 1:200; MS-113, Lab Vision Corporation, Fremont, CA, USA) overnight at 4°C, followed by incubation with a Histostain-*Plus* Kit according to the manufacturer's instructions (Zymed Laboratories, South San Francisco, CA, USA). The sections were routinely counterstained with hematoxylin. As immunohistochemical controls for immunostaining procedures, some sections were incubated with normal mouse IgG or PBS as a substitute for the primary antibody.

Morphometrical analysis was performed for a semi-quantitative evaluation of the immunohistochemical findings. The number of α-SMA$^+$ myofibroblasts within the injured sites was enumerated at 400-fold magnification in 6 random fields selected from each sample treated with JWH-133, AM-630 or Vehicle. Finally, the results were expressed as an average number.

Single immunofluorescence and confocal microscopy analysis

Briefly, deparaffinized sections without treatment were blocked with 5% BSA and incubated with mouse anti-α-SMA monoclonal antibodies (dilution 1:200; MS-113, Lab Vision Corporation, Fremont, CA, USA) overnight at 4°C. Thereafter, the sections were incubated with Alexa Fluor® 488 donkey anti-mouse IgG (dilution 1:200; A21202, Invitrogen, CA, USA) at room temperature for 2 h and protected from light. The nuclei were routinely counterstained with Hoechst 33258. Normal mouse IgG or PBS was used as an alternative to primary antibodies as the negative control. The sections were observed by confocal microscopy with the parameters described below.

A laser confocal scanning microscope system (FV1000S, Olympus, Japan), mounted on an inverted optical microscope (IX81, Olympus, Japan), was used. The observation and image acquisitions, using 20x and 60x oil immersion objective lenses, were performed via a 405-nm excitation/460-nm emission for the Hoechst 33258 and 488-nm excitation/519-nm emission for the Alexa Fluor® 488. In order to test for localization, a single section at the identical focus plane was scanned at a thickness of 0.62 μm in the z-axle, while the two channels were merged into a 12-bit RGB tif-file by employing FV1000 Viewer (Ver.1.6b) software. Following recording by confocal laser scanning microscopy, no alternations of the image files were performed by additional image processing.

Double indirect immunofluorescence and multichannel confocal microscopy analysis

Briefly, deparaffinized sections without treatment were blocked with 5% BSA, and incubated with rabbit anti-CB2R polyclonal antibodies (dilution 1:50; sc-25494, Santa Cruz Biotechnology, CA, USA) at room temperature for 2 h. The sections were further incubated with biotinylated donkey anti-rabbit IgG (dilution 1:200; ab6801, Abcam, Cambridge, UK) and streptavidin, Alexa Fluor® 555 conjugate (dilution 1:200; S-21381, Invitrogen, CA, USA). Following this, the tissue sections were then incubated with mouse anti-α-SMA monoclonal antibodies (dilution 1:200; MS-113, Lab Vision Corporation, Fremont, CA, USA) overnight at 4°C. After incubation with the Alexa Fluor® 488 donkey anti-mouse IgG (dilution 1:200; A21202, Invitrogen,

CA, USA) at room temperature for 2 h, the nuclei were routinely counterstained with Hoechst 33258. Normal rabbit or mouse IgG was used instead of primary antibodies as the negative control. Finally, the sections were observed by confocal microscopy with the parameters described below.

A laser confocal scanning microscope system (FV1000S, Olympus, Japan), mounted on an inverted optical microscope (IX81, Olympus, Japan), was used. The observation and image acquisitions, using a 60x oil immersion objective lens (numerical aperture 1.4), were performed via a 405-nm excitation/460-nm emission for Hoechst 33258, 488-nm excitation/519-nm emission for Alexa Fluor® 488 and 559-nm excitation/565-nm emission for Alexa Fluor® 555. In order to test for co-localization, a single section at the identical focus plane was scanned at a thickness of 0.62 µm in the z-axle, before the three channels were merged into a 12-bit RGB tif-file by utilizing FV1000 Viewer (Ver.1.6b) software. After recording through a confocal laser scanning microscopy, no alternations of the image files were performed by additional image processing.

Quantitative real-time reverse-transcriptase polymerase chain reaction (qRT-PCR) analysis

Total RNA was isolated from post-treated muscle specimens with RNAiso Plus (9108, Takara Biotechnology, Shiga, Japan) according to the manufacturer's instructions. The RNA concentration was assessed spectrophotometrically, and its integrity was checked by agarose gel electrophoresis. Reverse transcription of total RNA (1 µg) was performed using the PrimeScript™ RT reagent Kit (RR037A, Takara Biotechnology). As described in Table 1, the primers for the target and reference genes were designed and synthesized by Takara Biotechnology. Real-time fluorescence detection was conducted using an ABI PRISM® 7500 Real-Time PCR System (Applied Biosystems), while quantification was calculated using the comparative threshold cycle (Ct) method. The Ct of the duplicate measurements was used to calculate ΔCt as the difference in Ct between the target and reference genes. A relative quantity of product was expressed as fold-induction in JWH-133 or AM-630 treated samples, and then compared with the Vehicle-treated samples according to the formula 2-ΔΔCt, where ΔΔCt=ΔCt (JWH-133 or AM-630 sample) - ΔCt (Vehicle-treated sample) (Julien et al., 2005).

Statistical analysis

Data were expressed as means ± SEM and analyzed using SPSS for Windows 11.0. For comparisons among groups, the One-Way ANOVA was utilized for data analysis. A P value <0.05 was considered significant.

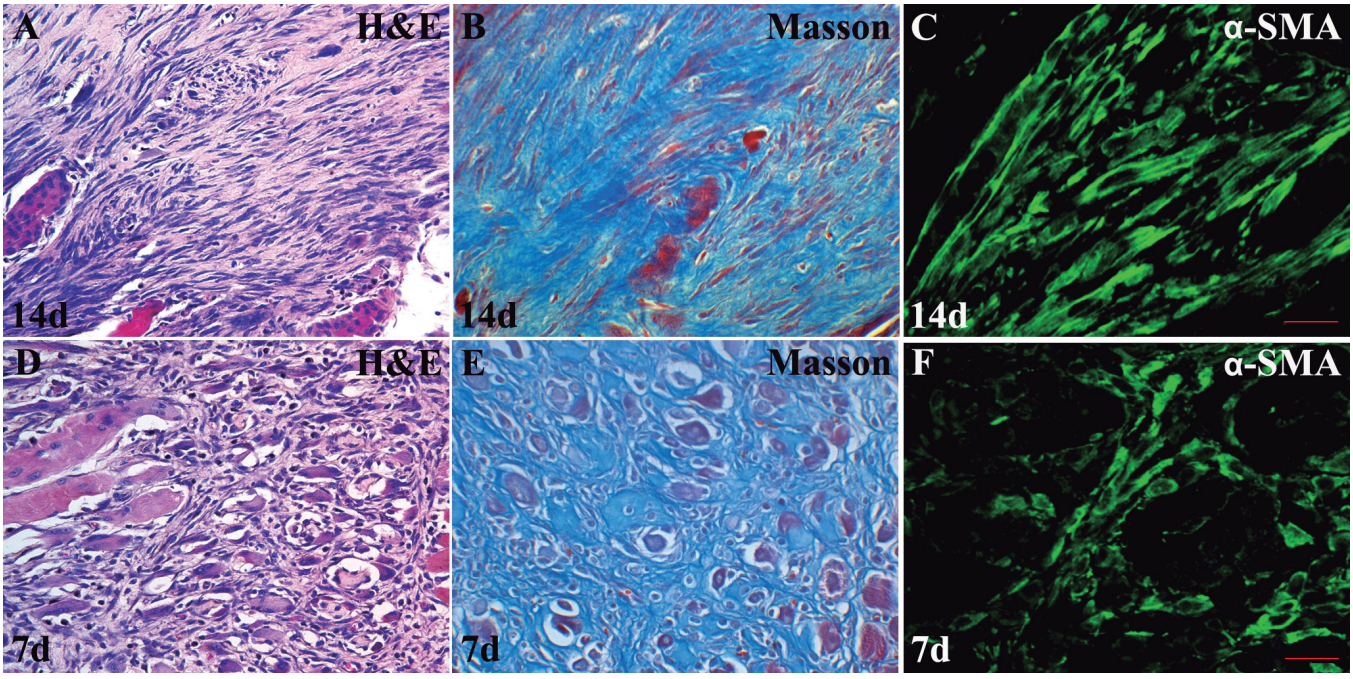

Fig. 1. A. The spindle-shaped fibroblastic cells (FBCs) were abundant at 14 days post-injury. **B.** Masson's trichrome staining was used to detect skeletal muscle fibrosis at 14 days post-injury. Large masses of collagen fibers were deposited in the injured sites. **C.** These myofibroblasts showed cytoplasmic immunoreactivity for α-SMA by confocal laser scanning microscopy. **D, E,** FBCs and collagen fibers surrounded regenerating myofibers at 7 days post-injury. **F.** The cytoplasm of myofibroblasts expressed α-SMA by confocal laser scanning microscopy. A, B, D, E, x 400; Scale bar: C, F, 10 µm.

Results

Our animal model creates obvious skeletal muscle injury and fibrosis

To study the anti-fibrosis effects of CB2R, we used a well-established animal model of skeletal muscle contusion to create skeletal muscle injury and fibrosis. The number of myofibroblasts and the collagen content at 14 days after injury were observed to reach a peak during the entire process of repair in injured skeletal muscle (data not shown). Therefore, it is conceivable that treatment with the CB2R agonist or antagonist prior to 14 days post-injury would be the most effective approach for regulating the severity of skeletal muscle fibrosis. In the present study, H&E staining provided the cornerstone for confirming the presence of skeletal muscle fibrosis at 14 days post-injury (Fig. 1A). Masson's trichrome staining was further used to stain collagen fibers. As shown in Fig. 1B,C, the spindle-shaped myofibroblasts' accumulation and collagen fibers' deposition were more abundant in injured sites at 14 days post-injury than at 7 days post-injury (Figs. 1D-F).

CB2R is induced in myofibroblasts after skeletal muscle injury without treatment

We first investigated whether CB2R is expressed in myofibroblasts after untreated skeletal muscle injury. Through double immunofluorescence, myofibroblasts were identified as a prominent cell type expressing CB2R in the injured sites. These myofibroblasts, with the appearance of a spindle-shaped morphology, showed

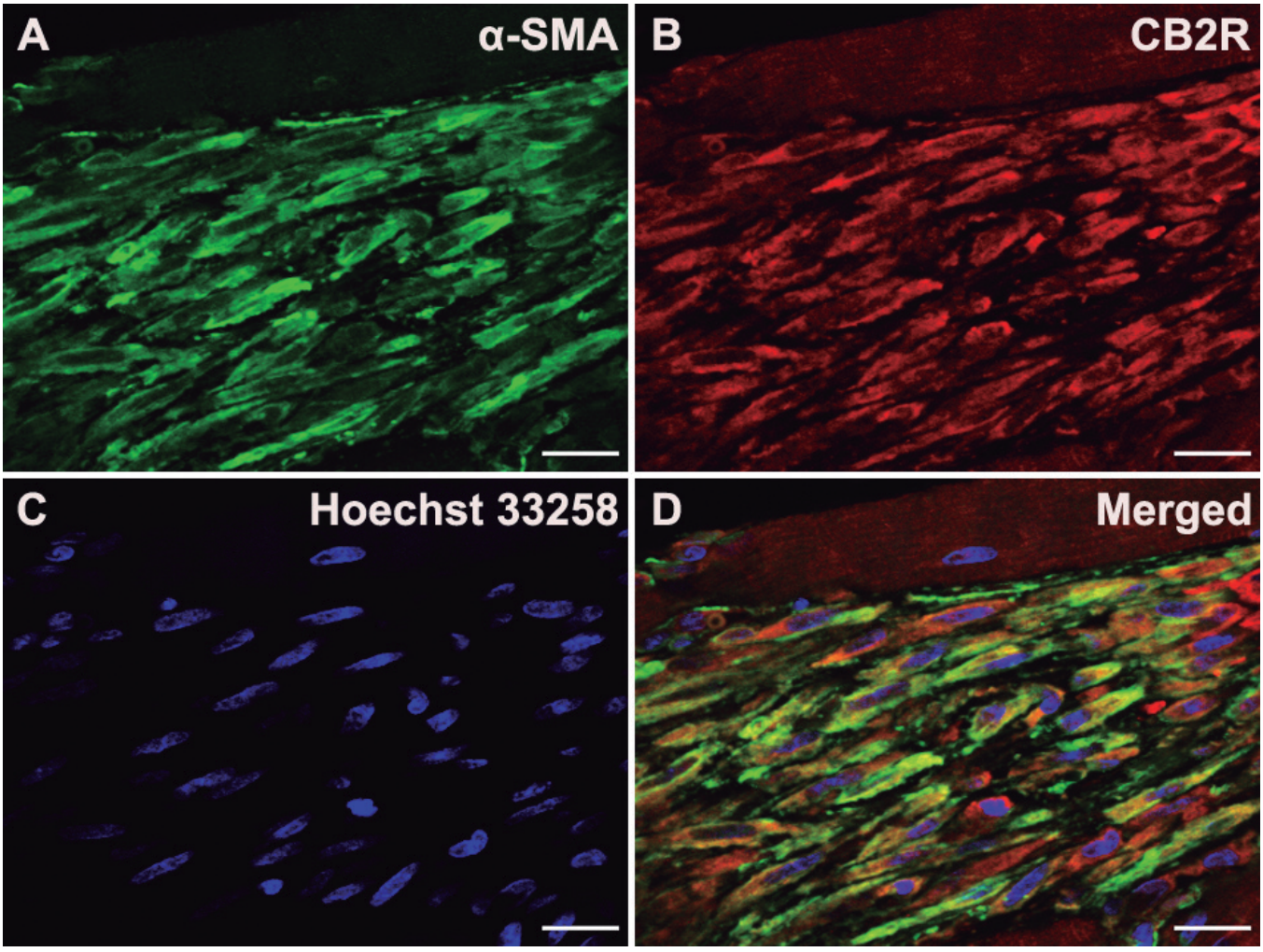

Fig. 2. Double indirect immunofluorescence analysis was performed to determine CB2R-expressing myofibroblasts at 14 days post-injury. The samples were immunostained with anti-α-SMA (**A**, green) and anti-CB2R (**B**, red). Image (**D**, yellow) of α-SMA and CB2R co-localization was digitally merged. Nuclei were counterstained with Hoechst 33258 (**C**, blue). Representative results from 5 individual experiments were shown here. Scale bars: 10 μm.

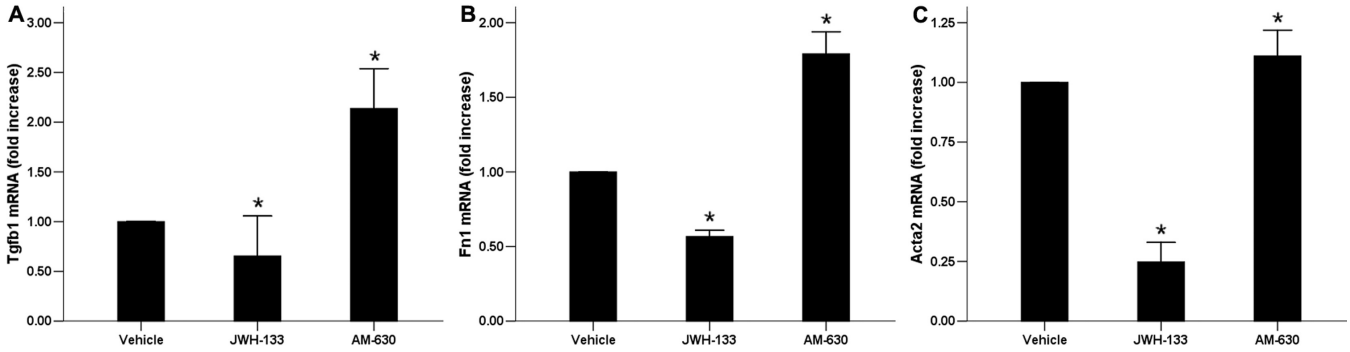

Fig. 3. The effects of CB2R agonist or antagonist on 3 fibrogenic markers by qRT-PCR in rats. JWH-133 abrogated the levels of Tgfb1 **(A)**, Fn1 **(B)** and Acta2 **(C)**. Nevertheless, AM-630 enhanced the levels of Tgfb1, Fn1 and Acta2. Values are means ± SEM of data. *P<0.05 (vs Vehicle).

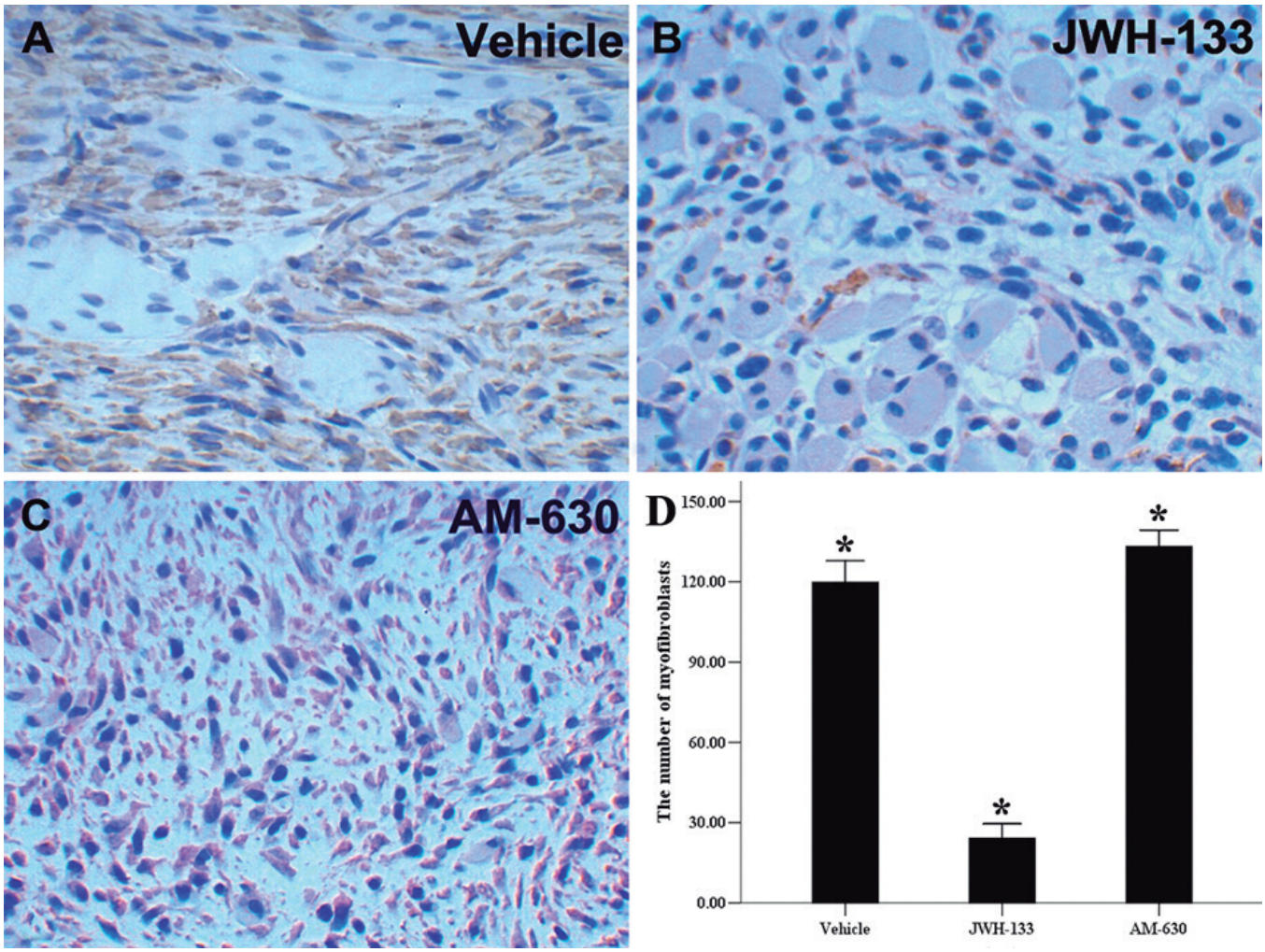

Fig. 4. Activation or inactivation of CB2R influenced on the number of myofibroblasts by immunohistochemical staining in rats. **A, C.** A large number of α-SMA-positive myofibroblasts segregated by ECM were present in the injured areas with Vehicle and AM-630 treatment. **B.** A few myofibroblasts were observed in the group treated with JWH-133. **D.** JWH-133 treatment decreased the number of myofibroblasts compared with Vehicle and AM-630. Values are means ± SEM of data. *P<0.05 (vs other groups). x 400

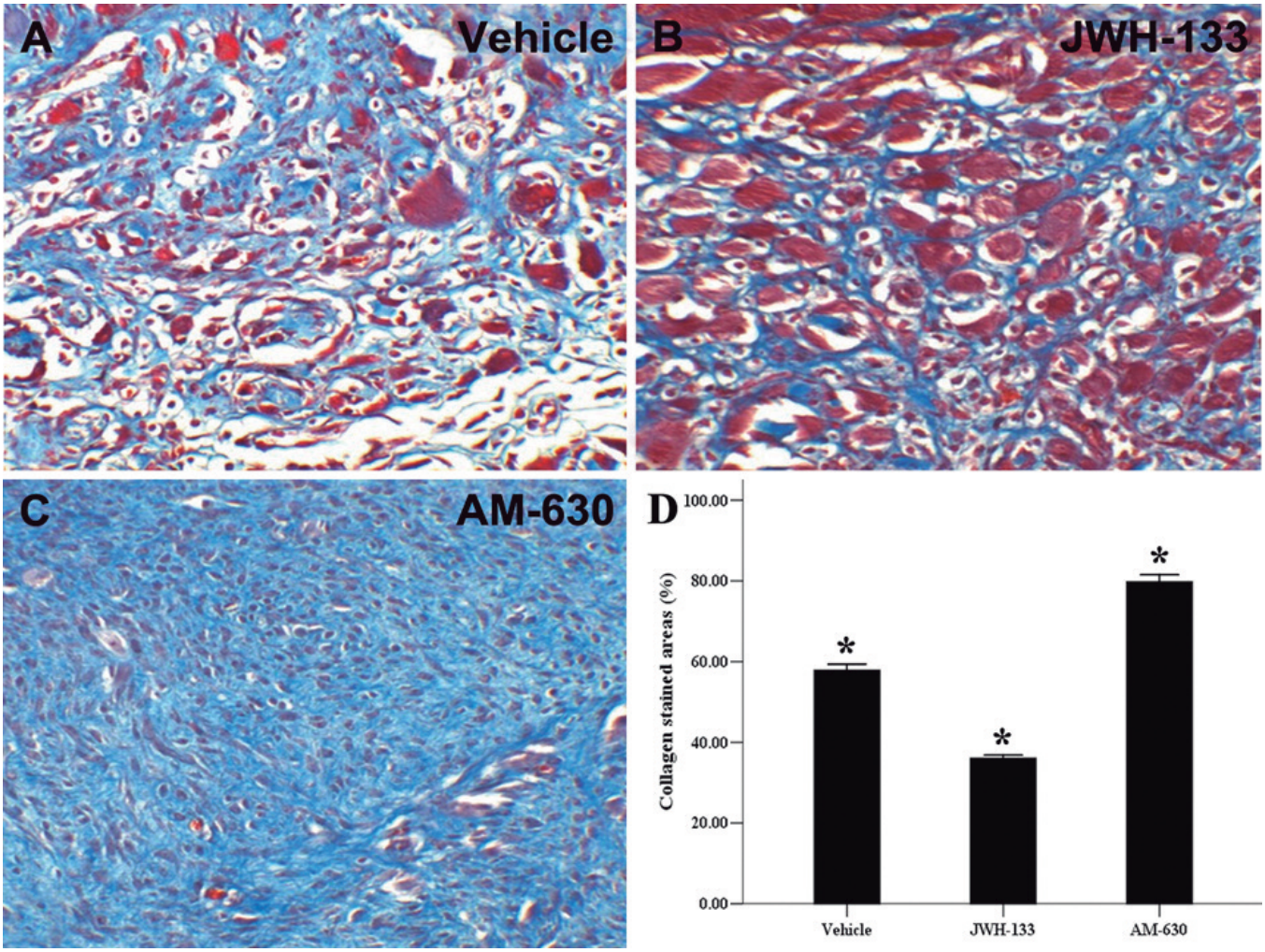

Fig. 5. CB2R activation or inactivation influenced the fibrotic extent by Masson's trichrome staining in rats. **A, B.** JWH-133-treated rats showed limited content of fibrosis and significantly fewer fibrotic areas than Vehicle-treated rats. **C.** AM-630-treated rats showed extensive areas of fibrosis in the injured areas. **D.** Treatment with AM-630 strongly increased fibrotic areas by 36.6% compared with rats treated with Vehicle. Nevertheless, fibrotic areas were decreased by 37.7% in JWH-133-treated rats compared with Vehicle-treated rats. Values are means ± SEM of data. *P<0.05 (vs other groups). x 400

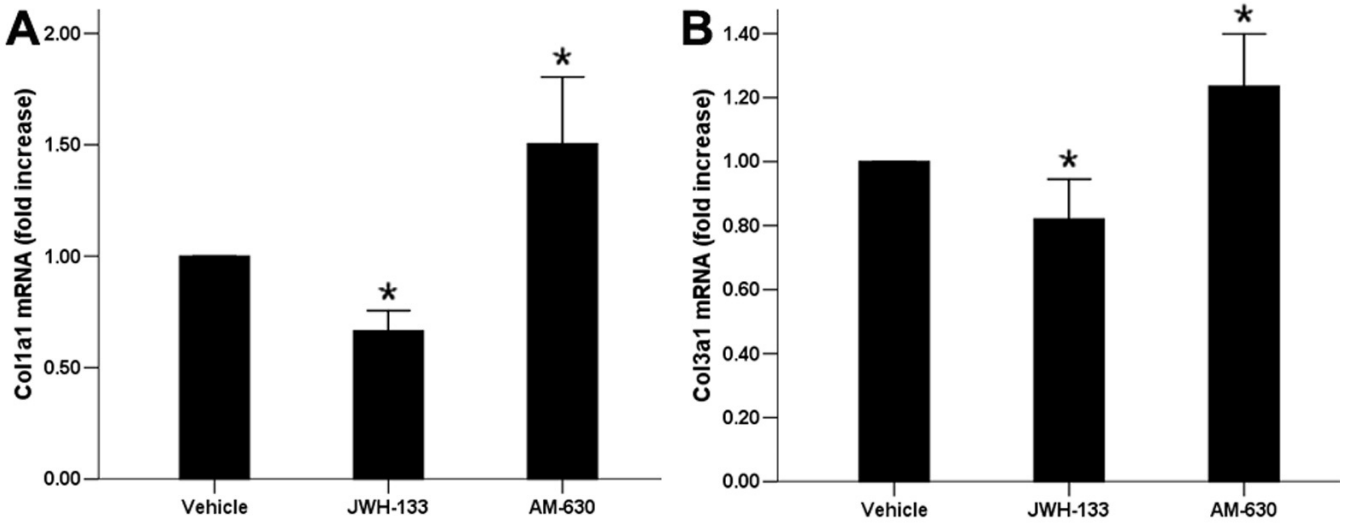

Fig. 6. The effects of CB2R agonist or antagonist on mRNA levels of Col I and Col III by qRT-PCR in rats. JWH-133 treatment decreased the levels of Col1a1 **(A)** and Col3a1 **(B)**. Nevertheless, AM-630 increased the levels of Col1a1 and Col3a1.Values are means ± SEM of data. *P<0.05 (vs Vehicle).

cytoplasmic immunoreactivity for CB2R and α-SMA (Fig. 2A-D).

CB2R prevents skeletal muscle fibrogenesis after injury

We next analyzed the effects of pharmacological activation or inactivation of CB2R on the induction of 3 fibrogenic markers: TGF-β1 (encoded by *Tgfb1*), FN-EIIIA (encoded by *Fn1*) and α-SMA (encoded by *Acta2*). The TGF-β1, FN-EIIIA and α-SMA mRNA were 0.65±0.16-fold, 0.57±0.02-fold and 0.25±0.03-fold lower in the JWH-133-treated rats as compared with those Vehicle-treated (P<0.05), respectively (Fig. 3A-C). Functional CB2R activation by the selective agonist JWH-133 significantly suppressed the expressions of *Tgfb1, Fn1* and *Acta2* in response to skeletal muscle injury. To further determine the role of CB2R in fibrogenesis during the repair of injured skeletal muscle, we performed local injections of AM-630, a selective CB2R antagonist, in contused rats. It was found that AM-630 significantly up-regulated the expressions of *Tgfb1, Fn1* and *Acta2* in comparison to Vehicle (Fig. 3A-C). Furthermore, rats receiving AM-630 were found to have greater numbers of myofibroblasts than those

Table 1. qRT-PCR primer sequences.

Gene	Primer		GenBank accession no.
Gapdh	Forward: Reverse:	5'-GGCACAGTCAAGGCTGAGAATG-3' 5'-ATGGTGGTGAAGACGCCAGTA-3'	NM_017008.3
Tgfb1	Forward: Reverse:	5'-TGCGCCTGCAGAGATTCAAG-3' 5'-AGGTAACGCCAGGAATTGTTGCTA-3'	NM_021578.2
Fn1	Forward: Reverse:	5'-GCACATGTCTCGGGAATGGA-3' 5'-ACACGTGCAGGAGCAAATGG-3'	NM_019143.2
Acta2	Forward: Reverse:	5'-AGCCAGTCGCCATCAGGAAC-3' 5'-CCGGAGCCATTGTCACACAC-3'	NM_031004.2
Col1a1	Forward: Reverse:	5'-GACATGTTCAGCTTTGTGGACCTC-3' 5'-AGGGACCCTTAGGCCATTGTG-3'	NM_053304.1
Col3a1	Forward: Reverse:	5'-ACATGATGAGCTTTGTGCAATGTG-3' 5'-ACCAAGGTAGTTGCATCCCAATTC-3'	NM_032085.1
Mmp1a	Forward: Reverse:	5'-CTGGCCAAATCTGCCAGGTAA-3' 5'-TCACAAACGGCAGCGTCAA-3'	NM_001134530.1
Mmp2	Forward: Reverse:	5'-CCAAGAACTTCCGACTATCCAATGA-3' 5'-CAGTGTAGGCGTGGGTCCAGTA-3'	NM_031054.2

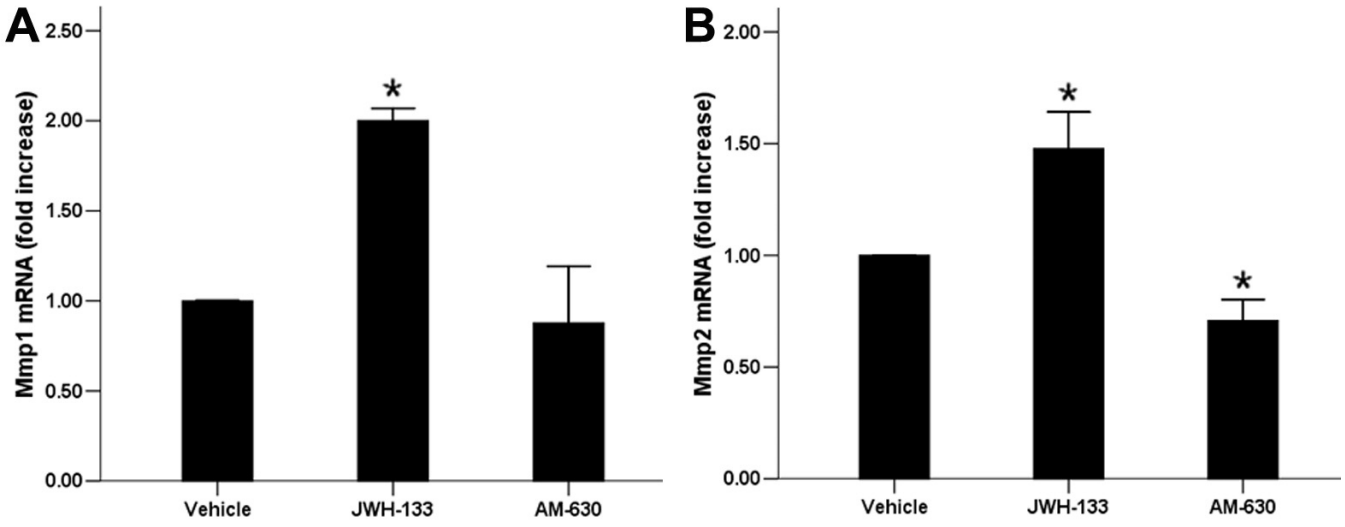

Fig. 7. The effects of CB2R agonist or antagonist on mRNA levels of MMP-1 and MMP-2 by qRT-PCR in rats. JWH-133 treatment augmented the levels of Mmp1 **(A)** and Mmp2 **(B)**. Nevertheless, AM-630 attenuated the levels of Mmp1 and Mmp2.Values are means ± SEM of data. *P<0.05 (vs Vehicle).

rats treated with JWH-133 and Vehicle (Fig. 4A-C) by morphometric analysis (Fig. 4D). As seen in Table 2, the average number of myofibroblasts increased following AM-630 treatment; however, delivery of JWH-133 induced a significant decrease in the average numbers of myofibroblasts.

In addition, JWH-133-treated rats presented significantly fewer fibrotic areas, which decreased by 37.7% (Fig. 5A,B,D). In contrast, more extensive fibrosis (which increased by 36.6%) was observed in the AM-630-treated rats than in the Vehicle-treated rats (Fig. 5A,C,D). The mRNA levels of collagen type I (encoded

Table 2. The number of myofibroblasts in Vehicle, JWH-133 and AM-630-treated groups (n=5, $\chi \pm S$).

Groups	The number of myofibroblasts
Vehicle	120±9.81*
JWH-133	24±6.62*
AM-630	133±7.57*

* P<0.05 vs other groups.

Table 3. The number of regenerating myofibers in Vehicle, JWH-133 and AM-630-treated groups (n=5, $\chi \pm S$).

Groups	The number of regenerating myofibers
Vehicle	41±4.09*
JWH-133	85±13.31*
AM-630	20±2.86*

* P<0.05 vs other groups.

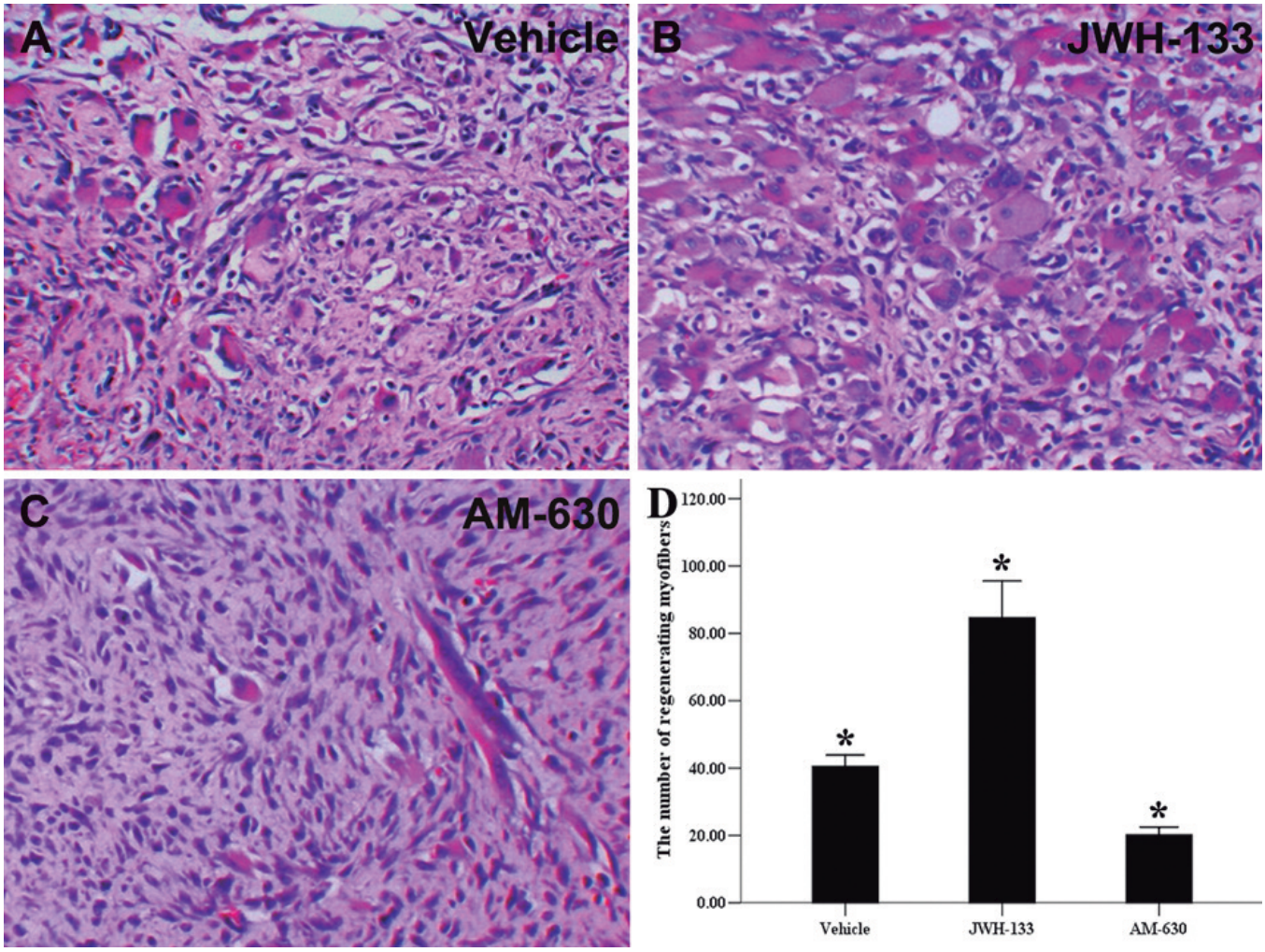

Fig. 8. CB2R activation or inactivation influenced on muscle regeneration by the H&E staining in rats. **A, C.** A few regenerating myofibers were observed in the injured sites of Vehicle and AM-630 groups. **B.** The majority of the injured sites in JWH-133-treated group was occupied by regenerating myofibers. **D.** JWH-133-treated group showed a significantly greater number of regenerating myofibers compared with other groups. Values are means ± SEM of data. *P<0.05 (vs other groups). x 400

by *Col1a1*) and collagen type III (encoded by *Col3a1*) in JWH-133-treated rats were significantly down-regulated as compared with rats treated with JWH-133 and Vehicle (Fig. 6A,B).

Overall, these results indicate that CB2R counteracted the development of fibrosis in response to skeletal muscle injury by decreasing mRNA levels of fibrogenic cytokines such as TGF-β1, FN-EIIIA and α-SMA, and reducing the accumulation of myofibroblasts.

CB2R regulates ECM remodeling after injury

To further clarify the effects of CB2R on ECM metabolism during the repair of injured skeletal muscle, MMP-1 (encoded by *Mmp1*) and MMP-2 (encoded by *Mmp2*) expressions were examined with JWH-133 or AM-630 by qRT-PCR analysis. Expressions of *Mmp1* and *Mmp2* were also significantly increased in JWH-133-treated rats when compared to the AM-630 and Vehicle-treated rats (Figs. 7A,B). Nevertheless, no significant change of *Mmp1* was detected with AM-630 compared to Vehicle, which somewhat differed from what had been anticipated. These results imply that the pharmacological agonism of CB2R might attenuate the fibrosis by degradation of ECM associated with skeletal muscle injury.

CB2R enhances muscle regeneration after injury

Finally, we investigated the influence of CB2R on muscle regeneration. As described in Fig. 8, regenerating myofibers with centrally located nuclei (multinucleated myofibers) were diffused distributed in the traumatized region for the Vehicle-treated rats (Fig. 8A). The regenerating myofibers significantly increased in number following the administration of JWH-133 (Fig. 8B), whereas only a small number of regenerating myofibers were observed, and these were occupied by fibrotic tissue and myofibroblastic cells in the rats treated with AM-630 (Fig. 8C). The quantity of centronucleated regenerating myofibers present in the injured sites was counted and compared among the three groups (Table 3), where the JWH-133-treated group showed a greater number of regenerating myofibers when compared with the other two groups (Fig. 8D), indicating that CB2R enhances muscle regeneration.

Discussion

In this article, we describe that JWH-133 delivered into the fibrotic area that develops following skeletal muscle injury resulted in dual therapeutic effects by both reducing residual collagen content and simultaneously increasing the number of regenerating myofibers. These results suggest that CB2R agonism could present a promising approach to overcoming muscular fibrosis after skeletal muscle injury.

Muscle contusion represents the major type of muscle injury, with more than 90% of muscle injuries being caused either by contusion or by excessive strain of the muscles. Our model of skeletal muscle contusion (by blunt impact to rat) mimics the characteristics of repair to injured skeletal muscle in humans, including skeletal muscle regeneration, myofibroblast infiltration and collagen deposition. Recently, several studies have demonstrated that CB2R can attenuate the extent of liver (Muñoz-Luque et al., 2008), cardiac (Defer et al., 2009), dermal (Akhmetshina et al., 2009), and pulmonary fibrosis (Servettaz et al., 2010). In concurrence with the results of the aforementioned studies, the administration of JWH-133 to rats using our model resulted in multiple beneficial effects by down-regulating the mRNA level of collagen type I, collagen type III, and decreasing the fibrotic areas in the traumatized skeletal muscles. Conversely, those rats treated with AM-630 increased in susceptibility to fibrosis.

Subsequently, we explored the reasons for the anti-fibrotic role of CB2R agonism after skeletal muscle injury *in vivo*. The fibrotic cascades after skeletal muscle injury include both fibrogenesis and the remodeling of ECM. During the initiation of fibrotic cascades, fibrogenesis is characterized by the up-regulation of fibrogenic marker TGF-β1, and myofibroblast hyperplasia. TGF-β1, which has previously been established in the fibrosis of other tissues (Bachem et al., 1993; Border and Noble, 1994; Bernasconi et al., 1995; Confalonieri et al., 1997; Dooley et al., 2000), is potentially also involved in muscle fibrosis post-muscle injury. TGF-β1 was also concomitant with the onset of muscle fibrosis in patients with either Duchenne's muscular dystrophy, a neuromuscular disease (Bernasconi et al., 1995), or chronic inflammatory muscle disease (Lundberg et al., 1997). CB2R activation by the selective agonist JWH-133 showed significantly decreased expressions of *Tgfb1*, as compared with Vehicle-treated rats. However, we obtained opposing results with respect to the AM-630-treated rats. In addition, the average number of myofibroblasts was 24±7.23 lower in the JWH-133-treated rats as compared with the other groups. These results suggest that the pharmacological agonism of CB2R reduced the fibrogenic response associated with skeletal muscle injury.

The reason that influenced the myofibroblast differentiation during the repair of skeletal muscle injury remains, however, incompletely elucidated. It was assumed previously that the resident fibroblasts were an important source of myofibroblasts by virtue of the differentiation through the 2 stages for fibrotic development in the skin, lungs and kidneys. The first step is that resident fibroblasts differentiate into the proto-myofibroblasts due to the mechanical stress the connective tissue experiences after a wound (Tomasek et al., 2002). Next, the proto-myofibroblasts are transdifferentiated into myofibroblasts by the combined action of TGF-β1 (Desmoulière et al., 1993; Rønnov-Jessen and Petersen, 1993) and the splice variant EIIIA of cellular fibronectin (Serini et al., 1998). In addition,

further study confirmed that muscle-derived stem cells (MC13 cells) with TGF-β1 stimulation expressed myofibroblastic markers, including α-SMA and vimentin, and that TGF-β1 could trigger differentiation of myoblasts into myofibroblasts both *in vivo* and *in vitro*, thereby leading to the advancement of fibrosis (Li et al., 2004). TGF-β1 is also capable of inducing the differentiation of bone marrow-derived fibrocytes (Abe et al., 2001; Kisseleva et al., 2006), and epithelial cells (Fan et al., 1999; Willis et al., 2005) into myofibroblasts in the fibrotic pathogenesis of the liver, kidneys and lungs. In the present study, we found that CB2R activation with JWH-133 decreased mRNA levels of TGF-β1 and FN-EIIIA, suggesting that that CB2R agonism might block TGF-β1 and FN-EIIIA triggered induction of the myofibroblastic phenotype, and accordingly reduce the number of myofibroblasts found in the injured sites.

Experimental studies demonstrated that suramin (Chan et al., 2003, 2005), decorin (Fukushima et al., 2001) and γ-interferon (Foster et al., 2003) could attenuate the extent of fibrosis in injured skeletal muscles by impeding key factors in the fibrotic cascade, such as TGF-β1, and ameliorate muscle regeneration. Nevertheless, related clinical applications were only effective if administered prior to fibrotic formation (Huard et al., 2003). In fact, the majority of patients who suffered from muscle injuries or neuromuscular disorders, such as Duchenne muscular dystrophy, only sought treatment after the formation of fibrosis in concomitance with the onset of affected limb pain and dysfunction. Therefore, a therapy that resolved fibrotic scarring during the advanced stage of fibrotic cascades would be more effective and practical. Matrix metalloproteinases (MMPs) are a family of zinc dependent proteolytic enzymes with the ability to cooperatively degrade all ECM components (Brinckerhoff and Matrisian, 2002). With late phasing in the fibrotic progression as ECM remodeling occurs, MMPs might play important roles in hindering myofibroblast adhesion to ECM, as has been suggested by studies on the regression of granulation tissue under a vascularized skin flap, and the resolution of liver fibrosis (Iredale et al., 1998; Darby et al., 2002). Moreover, the potential treatment of MMP-1 in fibrotic conditions was established by Iimuro et al. (2003), who employed the adenovirus recombinant proMMP-1 to treat liver fibrosis in a rat model. In the present study, rats treated with JWH-133 exemplified that up-regulation of MMP-1 and MMP-2 mRNA levels, while a significant decrease of *Mmp2* was detected with AM-630 compared to Vehicle and JWH-133. These results indicate that CB2R might be involved in ECM degradation during the repair of skeletal muscle injury.

As previously reported (Bedair et al., 2007; Kaar et al., 2008), proMMP-1 and active MMP-1 were capable of reducing collagen content to remove mechanical barriers, thereby facilitating muscle regeneration indirectly. A recent study further demonstrated that MMP-1 could enhance muscle regeneration by directly improving myoblast migration and differentiation *in vitro* and *in vivo* (Wang et al., 2009). In addition, over-expression of MMP-1 and MMP-2 have been shown to increase the migration and invasion of murine myoblasts in response to fibronectin *in vitro* (Allen et al., 2003). After muscle injuries satellite cells, located beneath the basement membrane of muscle fibers, become activated rapidly and MMP-2/-9 degrade the type IV collagen to facilitate the separation of the satellite cells from the basement membrane and their migration to the injured sites (Sires et al., 1993; Kherif et al., 1999). Our results highlighted that the number of regenerating myofibers was higher in the JWH-133-treated groups compared with the other groups, suggesting that JWH-133 administration effectively leads to enhanced muscle regeneration after muscle injury via the up-regulation of endogenous MMP-1/2. Our findings thus provide a clue to the intervention of fibrotic lesions in skeletal muscle functional disorder via CB2R agonism.

In summary, this study has described that CB2R was expressed in skeletal muscle myofibroblasts after injury. Moreover, owing to the use of CB2R agonist and antagonist, we have demonstrated for the first time that CB2R activation suppressed fibrotic progression and enhanced muscle regeneration, which may offer a new perspective on the treatment of skeletal muscle injuries and diseases.

Acknowledgements. This study was financially supported in part by grants from research funds for the Doctoral Program funded by Ministry of Education of China (200801590020) and National Natural Science Foundation of China (81202383) and Program for Young Innovative Research Team in China University of Political Science and Law.

References

Abe R., Donnelly S.C., Peng T., Bucala R. and Metz C.N. (2001). Peripheral blood fibrocytes: differentiation pathway and migration to wound sites. J. Immunol. 166, 7556-7562.

Akhmetshina A., Dees C., Busch N., Beer J., Sarter K., Zwerina J., Zimmer A., Distler O., Schett G. and Distler J.H. (2009). The cannabinoid receptor CB2 exerts antifibrotic effects in experimental dermal fibrosis. Arthritis Rheum. 60, 1129-1136.

Allen D.L., Teitelbaum D.H. and Kurachi K. (2003). Growth factor stimulation of matrix metalloproteinase expression and myoblast migration and invasion *in vitro*. Am. J. Physiol. 284, C805-C815.

Bachem M.G., Meyer D., Schäfer W., Riess U., Melchior R., Sell K.M. and Gressner A.M. (1993). The response of rat liver perisinusoidal lipocytes to polypeptide growth regulator changes with their transdifferentiation into myofibroblast-like cells in culture. J. Hepatol. 18, 40-52.

Bedair H., Liu T.T., Kaar J.L., Badlani S., Russell A.J., Li Y. and Huard J. (2007). Matrix metalloproteinase-1 therapy improves muscle healing. J. Appl. Physiol. 102, 2338-2345.

Bernasconi P., Torchiana E., Confalonieri P., Brugnoni R., Barresi R., Mora M., Cornelio F., Morandi L. and Mantegazza R. (1995). Expression of transforming growth factor-beta 1 in dystrophic patient

muscles correlates with fibrosis. Pathogenetic role of a fibrogenic cytokine. J. Clin. Invest. 96, 1137-1144.

Bisogno T., Ligresti A. and Di Marzo V. (2005). The endocannabinoid signalling system: Biochemical aspects. Pharmacol. Biochem. Behav. 81, 224-238.

Border W.A. and Noble N.A. (1994). Transforming growth factor beta in tissue fibrosis. N. Engl. J. Med. 10, 1286-1292.

Brinckerhoff C.E. and Matrisian L.M. (2002). Matrix metalloproteinases: a tail of a frog that became a prince. Nat. Rev. Mol. Cell. Biol. 3, 207-214.

Cavuoto P., McAinch A.J., Hatzinikolas G., Janovská A., Game P. and Wittert G.A. (2007). The expression of receptors for endocannabinoids in human and rodent skeletal muscle. Biochem. Biophys. Res. Commun. 364, 105-110.

Chan Y.S., Li Y., Foster W., Horaguchi T., Somogyi G., Fu F.H. and Huard J. (2003). Antifibrotic effects of suramin in injured skeletal muscle after laceration. J. Appl. Physiol. 95, 771-780.

Chan Y.S., Li Y., Foster W., Fu F.H. and Huard J. (2005). The use of suramin, an antifibrotic agent, to improve muscle recovery after strain injury. Am. J. Sports Med. 33, 43-51.

Confalonieri P., Bernasconi P., Cornelio F. and Mantegazza R. (1997). Transforming growth factor-beta 1 in polymyositis and dermatomyositis correlates with fibrosis but not with mononuclear cell infiltrate. J. Neuropathol. Exp. Neurol. 56, 479-484.

Darby IA., Bisucci T., Pittet B., Garbin S., Gabbiani G. and Desmoulière A. (2002). Skin flap-induced regression of granulation tissue correlates with reduced growth factor and increased metalloproteinase expression. J. Pathol. 197, 117-127.

Defer N., Wan J., Souktani R., Escoubet B., Perier M., Caramelle P., Manin S., Deveaux V., Bourin M.C., Zimmer A., Lotersztajn S., Pecker F. and Pavoine C. (2009). The cannabinoid receptor type 2 promotes cardiac myocyte and fibroblast survival and protects against ischemia/reperfusion-induced cardiomyopathy. FASEB J. 23, 2120-2130.

Desmoulière A., Geinoz A., Gabbiani F. and Gabbiani G. (1993). Transforming growth factor-beta 1 induces alpha-smooth muscle actin expression in granulation tissue myofibroblasts and in quiescent and growing cultured fibroblasts. J. Cell Biol. 122, 103-111.

Di Marzo V. (1998). 'Endocannabinoids' and other fatty acid derivatives with cannabimimetic properties: biochemistry and possible physiopathological relevance. Biochim. Biophys. Acta 1392, 153-175.

Dooley S., Delvoux B., Lahme B., Mangasser-Stephan K. and Gressner A.M. (2000). Modulation of transforming growth factor beta response and signaling during transdifferentiation of rat hepatic stellate cells to myofibroblasts. Hepatology 31, 1094-1106.

Fan J.M., Ng Y.Y., Hill P.A., Nikolic-Paterson D.J., Mu W., Atkins R.C. and Lan H.Y. (1999). Transforming growth factor-beta regulates tubular epithelial-myofibroblast transdifferentiation *in vitro*. Kidney. Int. 56, 1455-1467.

Felder C.C., Veluz J.S., Williams H.L., Briley E.M. and Matsuda L.A. (1992). Cannabinoid agonists stimulate both receptor- and non-receptor-mediated signal transduction pathways in cells transfected with and expressing cannabinoid receptor clones. Mol. Pharmacol. 42, 838-845.

Foster W., Li Y., Usas A., Somogyi G. and Huard J. (2003). Gamma interferon as an antifibrosis agent in skeletal muscle. J. Orthop. Res. 21, 798-804.

Fukushima K., Badlani N., Usas A., Riano F., Fu F. and Huard J. (2001). The use of an antifibrosis agent to improve muscle recovery after laceration. Am. J. Sports Med. 29, 394-402.

Goetsch S.C., Hawke TJ., Gallardo T.D., Richardson J.A. and Garry D.J. (2003). Transcriptional profiling and regulation of the extracellular matrix during muscle regeneration. Physiol. Genomics 14, 261-271.

Huard J., Li Y., Peng H. and Fu F.H. (2003). Gene therapy and tissue engineering for sports medicine. J. Gene. Med. 5, 93-108.

Iimuro Y., Nishio T., Morimoto T., Nitta T., Stefanovic B., Choi S.K., Brenner D.A. and Yamaoka Y. (2003). Delivery of matrix metalloproteinase-1 attenuates established liver fibrosis in the rate. Gastroenterology 124, 445-458.

Iredale J.P., Benyon R.C., Pickering J., McCullen M., Northrop M., Pawley S., Hovell C. and Arthur M.J. (1998). Mechanisms of spontaneous resolution of rat liver fibrosis. Hepatic stellate cell apoptosis and reduced hepatic expression of metalloproteinase inhibitors. J. Clin. Invest. 102, 538-549.

Julien B., Grenard P., Teixeira-Clerc F., Van Nhieu J.T., Li L., Karsak M., Zimmer A., Mallat A. and Lotersztajn S. (2005). Antifibrogenic role of the cannabinoid receptor CB2 in the liver. Gastroenterology 128, 742-755.

Kaar J.L., Li Y., Blair H.C., Asche G., Koepsel R.R., Huard J. and Russell A.J. (2008). Matrix metalloproteinase-1 treatment of muscle fibrosis. Acta Biomater. 4, 1411-1420.

Kherif S., Lafuma C., Dehaupas M., Lachkar S., Fournier J.G., Verdière-Sahuqué M., Fardeau M. and Alameddine HS. (1999). Expression of matrix metalloproteinases 2 and 9 in regenerating skeletal muscle: a study in experimentally injured and mdx muscles. Dev. Biol. 205, 158-170.

Kisseleva T., Uchinami H., Feirt N., Quintana-Bustamante O., Segovia J.C., Schwabe R.F. and Brenner D.A. (2006). Bone marrow-derived fibrocytes participate in pathogenesis of liver fibrosis. J. Hepatol. 45, 429-438.

Li Y., Foster W., Deasy BM., Chan Y., Prisk V., Tang Y., Cummins J. and Huard J. (2004). Transforming growth factor-beta1 induces the differentiation of myogenic cells into fibrotic cells in injured skeletal muscle: a key event in muscle fibrogenesis. Am. J. Pathol. 164, 1007-1019.

Lotersztajn S., Julien B., Teixeira-Clerc F., Grenard P. and Mallat A. (2005). Hepatic fibrosis: molecular mechanisms and drug targets. Annu. Rev. Pharmacol. Toxicol. 45, 605-628.

Lundberg I., Ulfgren A.K., Nyberg P., Andersson U. and Klareskog L. (1997). Cytokine production in muscle tissue of patients with idiopathic inflammatory myopathies. Arthritis Rheum. 40, 865-874.

Matsuda L.A., Lolait S.J., Brownstein M.J., Young AC. and Bonner T.I. (1990). Structure of a cannabinoid receptor and functional expression of the cloned cDNA. Nature 346, 561-564.

McAllister S.D. and Glass M. (2002). CB(1) and CB(2) receptor-mediated signalling: a focus on endocannabinoids. Prostaglandins. Leukot. Essent. Fatty Acids 66, 161-171.

Muñoz-Luque J., Ros J., Fernández-Varo G., Tugues S., Morales-Ruiz M., Alvarez C.E., Friedman SL., Arroyo V. and Jiménez W. (2008). Regression of fibrosis after chronic stimulation of cannabinoid CB2 receptor in cirrhotic rats. J. Pharmacol. Exp. Ther. 324, 475-483.

Munro S., Thomas K.L. and Abu-Shaar M. (1993). Molecular characterization of a peripheral receptor for cannabinoids. Nature 365, 61-65.

Pertwee R.G. (2001). Cannabinoid receptors and pain. Prog. Neurobiol.

63, 569-611.

Rønnov-Jessen L. and Petersen O.W. (1993). Induction of alpha-smooth muscle actin by transforming growth factor-beta 1 in quiescent human breast gland fibroblasts. Implications for myofibroblast generation in breast neoplasia. Lab. Invest. 68, 696-707.

Serini G., Bochaton-Piallat M.L., Ropraz P., Geinoz A., Borsi L., Zardi L. and Gabbiani G. (1998). The fibronectin domain ED-A is crucial for myofibroblastic phenotype induction by transforming growth factor-beta1. J. Cell Biol. 142, 873-881.

Servettaz A., Kavian N., Nicco C., Deveaux V., Chéreau C., Wang A., Zimmer A., Lotersztajn S., Weill B. and Batteux F. (2010). Targeting the cannabinoid pathway limits the development of fibrosis and autoimmunity in a mouse model of systemic sclerosis. Am. J. Pathol. 177, 187-196.

Sires U.I., Griffin G.L., Broekelmann T.J., Mecham R.P., Murphy G., Chung A.E., Welgus H.G. and Senior R.M. (1993). Degradation of entactin by matrix metalloproteinases. Susceptibility to matrilysin and identification of cleavage sites. J. Biol. Chem. 268, 2069-2074.

Tomasek J.J., Gabbiani G., Hinz B., Chaponnier C. and Brown R.A. (2002). Myofibroblasts and mechano-regulation of connective tissue remodelling. Nat. Rev. Mol. Cell. Biol. 3, 349-363.

Wang W., Pan H., Murray K., Jefferson B.S. and Li Y. (2009). Matrix metalloproteinase-1 promotes muscle cell migration and differentiation. Am. J. Pathol. 174, 541-549.

Willis B.C., Liebler J.M., Luby-Phelps K., Nicholson A.G., Crandall E.D., du Bois R.M. and Borok Z. (2005) Induction of epithelial-mesenchymal transition in alveolar epithelial cells by transforming growth factor-beta1: potential role in idiopathic pulmonary fibrosis. Am. J. Pathol. 166, 1321-1332.

Yu T.S., Cheng Z.H., Li L.Q., Zhao R., Fan Y.Y., Du Y., Ma W.X. and Guan D.W. (2010). The cannabinoid receptor type 2 is time-dependently expressed during skeletal muscle wound healing in rats. Int. J. Legal Med. 124, 397-404.

Zhang S.T., Zhao R., Ma W.X., Fan Y.Y., Guan W.Z., Wang J., Ren P., Zhong K., Yu T.S., Pi J.B. and Guan D.W. (2013). Nrf1 is time-dependently expressed and distributed in the distinct cell types after trauma to skeletal muscles in rats. Histol. Histopathol. 28, 725-735.

Accepeted January 15, 2015